
REPRESENTATION LEARNING IN A DECOMPOSED ENCODER DESIGN FOR BIO-INSPIRED HEBBIAN LEARNING

✉ **Achref Jaziri**

Department of Computer Science and Mathematics
Goethe University
60323 Frankfurt am Main, Germany
Jaziri@em.uni-frankfurt.de

Sina Ditzel

Department of Computer Science and Mathematics
Goethe University
60323 Frankfurt am Main, Germany
sina.ditzel@flandersmake.be

Iuliia Pliushch

Department of Educational Psychology
Goethe University
60629 Frankfurt am Main, Germany
pliushch@psych.uni-frankfurt.de

Visvanathan Ramesh

Department of Computer Science and Mathematics
Goethe University
60323 Frankfurt am Main, Germany
vramesh@em.uni-frankfurt.de

ABSTRACT

Modern data-driven machine learning system designs exploit inductive biases on architectural structure, invariance and equivariance requirements, task specific loss functions, and computational optimization tools. Previous works have illustrated that inductive bias in the early layers of the encoder in the form of human specified quasi-invariant filters can serve as a powerful inductive bias to attain better robustness and transparency in learned classifiers. This paper explores this further in the context of representation learning with local plasticity rules i.e. bio-inspired Hebbian learning. We propose a modular framework trained with a bio-inspired variant of contrastive predictive coding (Hinge CLAPP Loss). Our framework is composed of parallel encoders each leveraging a different invariant visual descriptor as an inductive bias. We evaluate the representation learning capacity of our system in a classification scenario on image data of various difficulties (GTSRB, STL10, CODEBRIM) as well as video data (UCF101). Our findings indicate that this form of inductive bias can be beneficial in closing the gap between models with local plasticity rules and backpropagation models as well as learning more robust representations in general.

Keywords Representation Learning · Hebbian Learning · Invariances · Contrastive Learning

1 Introduction

Computer vision tasks often involve invariance to nuisance variables such as object pose, size, illumination conditions, etc. In the late 80's and 90's, involving expert driven model-based design, this has been achieved by stacking and combining quasi-invariant transformations which guarantee that the output remains unchanged for a range of transformations that are irrelevant to the current context Binford and Levitt [1993], Chin and Dyer [1986].

Modern machine learning uses deep neural networks (DNN) to learn implicit transformations from data instead of explicitly defining invariance requirements upfront Bengio [2009], Krizhevsky et al. [2012], LeCun et al. [2004]. DNNs have shown to be highly effective in many application scenarios. Nevertheless due to their black box nature, it is difficult to pinpoint precisely which types of invariances were learned and what image features were leveraged by the network during decision making. Recently, symmetries in neural networks as inductive bias gained attention and ways to discover these have been proposed Moskalev et al. [2022], Liu and Tegmark [2022]. In sum, the lack of transparency coupled with the brittleness to adversarial perturbations are some of the main challenges of machine learning design Barredo Arrieta et al. [2020], Carvalho et al. [2019].

One way to gain more understanding into the inner-workings of a neural networks-based system is through decomposable design Lipton [2016]. The efforts in the 90's on quasi-invariance may be seen as a form of decomposition that allows for efficient generation of hypotheses for matching Binford and Levitt [1993]. Essentially, the appropriate choice of invariant operators for a given application context enables one to disregard nuisance variables that are irrelevant to the task on hand. This aspect of exploiting generative models defined by the modeler to specify choice of invariant operators and characterizing the statistical properties of the operator as a function of noise models has been discussed in the context of performance characterization frameworks for computer vision Thacker et al. [2008]. A promising direction, combining benefits of model-based and deep-learning approaches, is to both leverage knowledge about the task in the form of inductive biases and learn the parts which are difficult to model. Baslamisli et al. [2021], for example, define albedo and shading gradient descriptors using physics-based models and refine the initial estimates using a decomposed albedo/shading encoder-decoder architecture with fusion.

Inductive bias for invariant operator selection may come from physics-based generative models, mathematical arguments or from neuroscience. For example, Luan et al. [2018], Pérez et al. [2020] have illustrated that inductive bias in the early layers of the encoder in the form of human specified (quasi-)invariant filters, e.g. Gabor filters, can serve as a powerful tool to attain a more robust performance in learned classifiers, making the neural network design more transparent and explainable. Parallels can be drawn between the design of decomposable vision systems and brain-inspired vision architectures. The visual system of mammals consists of parallel, hierarchical specialized pathways, interpreting different parts of the input signals Ungerleider [1982]. Various proposals for brain-inspired architectures draw inspiration from these structures and present decomposable systems that process multiple cues such as color, shape, texture in parallel with specialized pathways von der Malsburg [2014], Hinton [2021], Hawkins et al. [2019].

Learning in the primate brain is thought to occur in an unsupervised manner according to local plasticity rules Hebb [1949]. Previous works are seeking to extend neural networks with local brain-inspired learning rule to replace backpropagation Pogodin and Latham [2020], Lillicrap et al. [2016], Oja [1982]. The main motivation of this line of research is understanding how learning happens in the brain, which has the potential to alleviate learning in artificial intelligent systems as well as learn more efficiently with less computational resources Wunderlich et al. [2019]. However, the performance of neural networks trained with current bio-inspired rules is usually worse than standard backpropagation networks on the same tasks Bartunov et al. [2018].

In this work, we posit that integrating local plasticity rules in a modular decomposable structure can be beneficial in further closing the gap to networks trained with backpropagation. Inspired by previous works that argue that learning in biological systems does not happen on a blank slate Zador [2019], we explore the combination of these two perspectives: inductive bias in the form of visual invariant operators, motivated from physics and mathematical analyses, for disentanglement and biologically inspired local learning. We present a framework composed of multiple encoder networks each one of them is extended with a different invariant visual descriptor (e.g red-green normalization, local binary pattern operator and dual-tree complex wavelet transform). The neural networks are trained under a contrastive loss in a self-supervised fashion. For video data, we design an additional encoder trained in a self-supervised setting to learn motion sensitive representations. We validate the learned representations with a linear classifier on image (GTSRB, STL10, CODEBRIM) and video (UCF101) data. Our findings provide evidence that better classification of learned representations can be achieved by a judicious choice of inductive biases for decomposition.

2 Related Work

Disentanglement: Disentanglement is a broad concept, familiar nowadays in the first place due to the discussion on how -VAEs can disentangle generative factors of variations in the latent space Higgins et al. [2017, 2022] and when they fail to do so Locatello et al. [2019]. More generally though, it can be understood as a *decomposition*, namely imposing the desired structure in the latent space Mathieu et al. [2019]. In this sense, modularization of the generative model by using the knowledge about the data generation process as in Niemeyer and Geiger [2021], Nguyen-Phuoc et al. [2019] can also be called disentanglement. Understanding which causal factors generated the data, as well as the knowledge of the task at hand, determine how best to (pre-)process them, e.g. whether illumination or texture is relevant for the given task. We analyze the classification performance of neural networks, consisting of several encoders, each preceded by a certain preprocessing step using visual descriptors such as LBP, color transformations or wavelets. The data is in this way transformed into a suitable feature space to solve the task(s). Several transformations may be important for the same task, but the benefit of decomposition is that the influence of every transformation can be analyzed separately. Generalizations can hence be made regarding which types of data are to be preprocessed in which way. In neural networks, the choice of these quasi-operators is learned implicitly during training. Explicit design of transform operators requires a versatile domain knowledge about the input data, but by building a decomposition pipeline with different preprocessing operators one could also automatize the process of finding out, what is relevant in the data for the given task.

Combination of Invariant Visual Descriptors and Neural Architectures: Various works attempt to create less opaque and more robust pipelines by integrating well-understood operators into data-driven pipelines. For instance, the SIFT detector, which is quasi-invariant to scale, orientation and illumination, was used in combination with a neural architecture Perronnin and Larlus [2015]. Based on the Local-Binary Pattern (LBP) operator an adapted convolutional layer with less parameters was proposed that extracts texture features Juefei-Xu et al. [2017], Lin et al. [2020] Lin et al. [2020]. Taking strong inspiration from findings on primate vision, evidence has been put forward that fixing the first layers of a convolutional neural network (CNN) to simulate the image processing of the primate primary visual cortex benefits robustness towards input perturbations and adversarial attacks Dapello et al. [2020]. Scattering transforms preserve high frequency information and are invariant to geometric transformations and stable to deformations. Comparable performance on classification benchmarks to pure CNN’s has been shown, while using less parameter and providing more theoretical guarantees Oyallon et al. [2017]. Li et al. [2020] improved noise-robustness classification accuracy in CNN by replacing down-sampling layers with discrete wavelet transforms.

The former works focus on a single most robust, or most discriminating operator respectively, and train the data-driven part of the model in a supervised manner. Our work investigates the combination of multiple self-supervised neural encoders, each combined with an invariant operator. Explicitly, we use three quasi-invariants, one texture operator (LBP), one color transformation (rg normalization), as well as, a frequency-related operator (wavelets).

Representation Learning/ Contrastive Learning: Learning generalizable features has been attempted by self-supervised learning, which is concerned with the extraction of patterns from data in the absence of labels. Instead of labels, a certain pretext task, for example image inpainting, image colorization or clustering based on pseudo-labels, can be used to shape the representation space Jing and Tian [2019]. Mapping the representations of similar instances closer together in the feature space than dissimilar instances can also directly be achieved by contrastive learning Le-Khac et al. [2020]. Data augmentations are often used to generate pairs of such similar images, deciding which invariances are learned. Which augmentations work in which context and why is still subject of research though. Recent works have explored contrastive learning in the context of bio-inspired learning Illing et al. [2021], et al. [2022]. In our work, we show that we can improve representation learning by integrating well understood visual descriptors to learn more disentangled representation.

Biologically Inspired Learning: Unlike backpropagation updates, Hebbian plasticity rules are local and depend only on the activations of the pre- and post-synaptic neurons and usually a third modulation factor related to reward or other high level signals. There is also a growing body of works in the literature that leverage local plasticity rules to train deep neural networks Bengio [2009], Illing et al. [2021], Krotov and Hopfield [2019], Nøklund and Eidnes [2019], Pogodin and Latham [2020], Xie and Seung [2003], Millidge et al. [2022]. Alternatives for backpropagation include systems that decouple the feedforward and feedback network paths to circumvent some of the biologically implausible aspects of backpropagation Amit [2019], Lillicrap et al. [2016], Crafton et al. [2019], Han and Yoo [2019], Moskovitz et al. [2018], Nøklund [2016].

The imposed constraints on gradient propagation usually come with decrease in downstream task performance. Despite recent advances, scaling beyond simple image classification benchmarks remains an issue for bio-inspired systems Bartunov et al. [2018]. There are open questions about the merits of using local rules for training deep learning architectures. Some works showed in fact better data efficiency with local Hebbian training Lagani et al. [2021] or more sparse representations Földiák [1990]. But generally, the properties of networks trained with local learning rules, especially in the current age of big data-driven systems, are not well understood.

This paper argues that the performance gap of bio-inspired learning rule can be addressed with appropriate network structures and inductive biases. We analyze the representation learning capacity of our framework on classification tasks of various difficulties including in a multi-label setting and show that the framework variant with local plasticity rules benefits the most from this structure which helps in closing the gap to backpropagation models.

3 Method

3.1 Decomposition

We explore the decomposition of the input signal using operators with well established properties: wavelet transform, rg normalization and Local Binary Pattern (LBP) (Figure 1). Each extracted representation is sensitive to different features in the image, hence decomposing into different invariant spaces. These operators serve as inductive biases to learn invariant latent representations. We hypothesize that our approach will help leverage quasi-invariant spaces and learn more robust, stable and generalizable representations, particularly in the context of local plasticity rules where the signal cannot be backpropagated across the whole model.

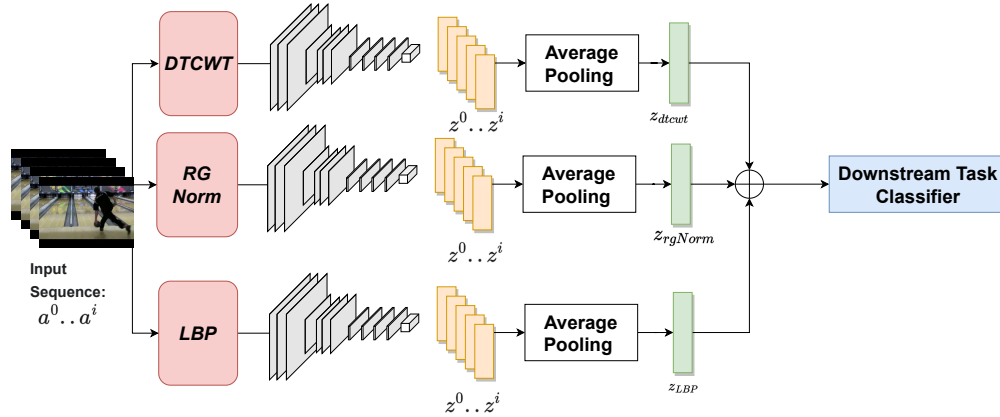


Figure 1: An illustration of the presented framework. Each encoder network is preceded by a transformation and is trained in a contrastive learning setting. Afterwards, the linear classifier is trained on a downstream classification task while the weights of the encoders are frozen.

LBP: Local Binary Pattern (LBP) is a visual descriptor that describes the local texture patterns of an image Ojala et al. [2002]. LBP assigns a value to each pixel in an image by comparing its intensity with the values of neighboring pixels and then assigning a binary number based on the comparison. LBP is a popular operator in various application domains like face recognition or texture analysis due to its robustness to illumination changes as well as its computational simplicity Maenpaa [2004], Ahonen et al. [2006]. When an image is rotated, the indexes of the different neighbouring pixels change which results in different LBP values. Maenpaa [2004] suggests that by circularly rotating the neighbouring pixels until a minimum value for the binary number is obtained, the LBP values stay the same independent of the current rotation of the input image. We use this version of LBP in our experiments.

RG Normalization: To obtain color values without intensity information, it is possible to transform RGB channels of an image to a normalized rg space Gevers and Smeulders [1999]. This is helpful to reduce the effect of varying illumination levels onto the task. The normalized rg values can be computed in the following way:

$$r_{norm} = \frac{R}{R + G + B} \quad g_{norm} = \frac{G}{R + G + B} \quad (1)$$

Wavelet Transform: The third decomposition operator that we consider is Dual Tree Complex Wavelet Transform (DTCWT). It is an enhancement of the discrete wavelet transform (DWT) providing better shift invariance Kingsbury [1998]. Unlike Fourier transforms which only capture the frequency, discrete wavelet transforms captures both frequency and location in time. DTCWT bears many similarities to the Morlet transform used in the invariant scattering convolution networks Bruna and Mallat [2013]. We refer to Valens [1999] for a detailed theory of different wavelet transforms and their respective advantages.

Motion-sensitive Encoder for Video: For video data, we further extend our framework with an additional encoder (MovNet). MovNet is trained with a self-supervised objective for the discrimination between pseudo-egomotion and scene motion in video. Egomotion can be understood as the motion of the observer or the camera, while scene motion is the motion of the objects in a video scene. Further details about the encoder can be found in section 4.7 and Figure 4.

3.2 Local Learning with Contrastive Predictive Coding

We consider training the encoders in a contrastive predictive coding (CPC) setting before concatenating their extracted representations for downstream tasks. More details about CPC can be found in this paper Oord et al. [2018]. The main idea is that the encoder extracts useful representations from a sequence of inputs (e.g sequence of video frames or a sequence of image patches) by learning to predict the future response (an image patch or video frame) in latent space, while at the same time keeping the prediction as far as possible from the responses to negative examples.

A follow-up paper Illing et al. [2021] interprets this future response as a fixation of gaze or as a saccade movement, shifting the center of gaze. The main intuition is that for continuous input streams, the statistics of consecutive frames should have similar latent representations as long as there is a fixation of the eye movement on the same object/scene. In this biologically inspired setting, Contrastive, Local And Predictive Plasticity (CLAPP) Illing et al. [2021] model

uses a Hinge loss to train an encoder layer-wise via a Hebbian-like learning rule. The role of Hinge loss is to contrast representations with each other. We use this bio-inspired CLAPP model with local learning for our experiments. In further accordance with Illing et al. [2021], we will also compare the above Hebbian version with a CPC variant using the same Hinge loss but trained end-to-end. This we will refer to as HingeCPC.

In the case of image data, the sequence needed for self-supervision is created by dividing the images patch-wise Oord et al. [2018], Illing et al. [2021]. The patches overlap to simulate a sequence of movements from a single image and are stored in a batch in vertical order of the image. Given a sequence of input patches from several images, the encoder network produces a representation z^t for each time step t (for every patch). Each of the patches can be interpreted as a *context* for other patches, determining whether they stem from a continuous scene. The context could in principle encompass several previous time steps, for simplification here $c^t = z^t$. Specifically, a *context* representation c^t at time t is used to predict the representations of encoded image patches at future time steps $t + \delta$, up to 5 patches into the future. This means that c^t is used to predict the representations $z^{t+\delta}$ for $\delta \in \{1..5\}$, where these representations might be encoded patches from the same image (or frames taken from the same video) - positive examples, or randomly sampled patches from other images within the same batch - negative examples. A linear transformation matrix W^{pred} is used for the prediction:

$$z_{pred}^t = W^{pred} \cdot c^t \quad (2)$$

The obtained predictions for future time steps z_{pred}^t are either aligned with the actual representations computed by the encoder $z^{t+\delta}$ for positive examples, or contrasted in case of a negative ones, using a Hinge loss function:

$$L^t = \max(0, 1 - y^t \cdot z^{t+\delta} \cdot z_{pred}^t) \quad (3)$$

y^t is the global modulation signal and can be viewed as the label of a binary classification problem characterized by the Hinge loss. If we have a positive example then $y^t = 1$ and in the case of a negative example $y^t = -1$.

Hinge loss can either be applied to the last layer and trained with backpropagation (HingeCPC) or computed for each layer separately. By applying this loss objective layer-wise, learning can proceed based on local information (CLAPP) without the need for top-down feedback as used in backpropagation. CLAPP'S weight update is Hebbian, which only depends on local information available to that layer and a global modulation signal y^t .

4 Experiments

4.1 Experimental Setting

Datasets: To evaluate our models, we use primarily two standard classification benchmarks (GTSRB and STL10) and one multi-target classification dataset of concrete defects CODEBRIM as well as an action recognition video dataset UCF101. GTSRB refers to the German Traffic Sign Recognition Benchmark Stallkamp et al. [2011]. It contains images of 43 different traffic sign classes, extracted from video recordings under different light and weather conditions. The street sign appearance makes them easy to identify for humans, because of well-defined discriminative features of color, shape, symbols and text. The dataset contains 39,209 training images and 12,630 test images. We use the same training set for both self-supervised encoder training and supervised classifier training.

The STL-10 dataset is an image recognition dataset for unsupervised feature learning Coates et al. [2011], similar to CIFAR10. However, each class has fewer labeled training examples than in CIFAR-10, but a very large set of unlabeled examples for unsupervised learning. The number of unlabeled images is around 100000 whereas the number of labeled images is around 5000. The test set is composed of 800 images for each of the 10 classes. The classes of objects present in the dataset are: airplane, bird, car, cat, deer, dog, horse, monkey, ship, truck.

CODEBRIM is a multi-target classification dataset of defects on concrete surfaces Mundt et al. [2019] with 5 classes of defects: crack, spallation, efflorescence, exposed bars and corrosion stains. It is possible to have multiple defects in the same image. This is a major difference to other benchmarks. CODEBRIM not only allows us to validate our design in a practical real world setting but also investigate if it is possible to infer multiple objects from the latent space extracted by our self-supervised models. The dataset also contains varied and challenging cases due to the overlapping defects, varied appearance of concrete surfaces, presence of surface markings and varied weather conditions. The training set contains 5354 defect bounding boxes with at least one defect and 2506 background bounding boxes of 30 unique bridges, acquired at different scales at a high resolutions. The test set contains 150 defect examples per class.

UCF101 is a standard action recognition dataset to evaluate 3D models and is composed of realistic action videos categorized in 101 action categories Soomro et al. [2012].

Method	GTSRB		STL10	
	Accuracy	Difference	Accuracy	Difference
Supervised VGG	97.4 ± 0.42	-	75.47 ± 0.03	-
HingeCPC Illing et al. [2021], Oord et al. [2018]	84.2 ± 0.7	-	69.18 ± 0.07	-
CLAPP Illing et al. [2021]	79.61 ± 0.81	-	66.61 ± 0.28	-
<i>LBP</i> + HingeCPC	94.8 ± 0.46	+10.6	53.52 ± 0.12	-15.66
<i>RGNorm</i> + HingeCPC	35.78 ± 0.16	-48.42	46.24 ± 0.49	-22.94
<i>DTCWT</i> + HingeCPC	77.44 ± 0.6	-6.76	71.44 ± 0.01	+2.26
<i>LBP</i> + CLAPP	94.2 ± 0.34	+14.5	55.35 ± 3.44	-11.26
<i>RGNorm</i> + CLAPP	33.78 ± 0.45	-45.83	45.59 ± 1.45	-21.02
<i>DTCWT</i> + CLAPP	76.1 ± 0.51	-3.51	69.37 ± 0.01	+2.76
ours (Backprop)	94.83 ± 0.55	+10.63	74.13 ± 0.05	+4.95
ours (Local)	94.21 ± 0.24	+14.6	72.97 ± 0.02	+6.36

Table 1: Performance comparison in terms of classification accuracy (%). The best performing self-supervised model is highlighted in red, in bold the best performing model for each category: baselines, models trained with HingeCPC, models trained with CLAPP, decomposed encoders. The difference column contains the performance gap between the model and its baseline, which is HingeCPC for encoders trained with backpropagation and CLAPP for encoders trained with local plasticity rule.

Training Details and Hyperparameters: Our encoders are 6-layer-CNNs trained in parallel (see appendix for architecture details). We have two versions of our proposed method: one trained with local learning rule (**ours(Local)**) and the other one trained with backpropagation (**ours(Backprop)**).

For comparison, we consider three baseline models: end-to-end supervised classification learning (Supervised-VGG), training with local plasticity rules for contrastive predictive coding (CLAPP) and backpropagation training with Hinge loss formulation for contrastive predictive coding (HingeCPC) Illing et al. [2021]. For local training, each layer is trained greedily with the loss objective.

The encoders are implemented in Pytorch and trained on two A100 Nvidia GPUs using Adam with an initial learning rate of 10^{-5} and weight decay of $5 \cdot 10^{-6}$, mini-batch size 64, where each image is randomly cropped and downsized to 64x64 resolution. We also perform some random flipping of the images with probability $p = 0.5$ during training to augment the data. All encoders are trained for 200 epochs. To simulate a sequence of frames for static images, each image is split into patches of size 16x16, similar to Illing et al. [2021], Löwe et al. [2019].

For video data, sequences of 16 frames taken from UCF101 videos are used instead of patches. For training, we use the same hyperparameters as the experiments on image data except a smaller batch size of 16 and 400 instead of 200 epochs. The frames in each video sequence have a resolution of 120x120.

Evaluation Procedure: To quantitatively evaluate the quality of learned representations, we train a linear classifier to recognize the class labels of each dataset while freezing the trained encoder(s). The image patches/video frames are viewed one after the other by the frozen encoders. After that, we perform average pooling over the patch representations to obtain a single representation vector for an input image or video. This vector is then passed to the classifier network. In the case of a multi-encoder setting, the representation vectors of different encoders are concatenated before passing them to the classifier. The linear classifier is composed of two fully connected layers and a dropout layers with $p = 0.5$. See appendix for further details.

4.2 Experimental Results

The empirical results for classification task on STL10 and GTSRB are found in table 1. Both versions of our method (Backprop and Local) achieve a performance closer to that of the supervised models. Ours(Local) sees a 14.6% performance improvement on GTSRB and 6.36% on STL10 compared to CLAPP, i.e a local learning variant without decomposition. Interestingly, the improvement due to decomposition is higher for local learning than for the layer-wise backpropagation: ours(Backprop) improves only by 10.63% in comparison to HingeCPC.

Hence, decomposition seems to help close the gap between learning with local plasticity rules and learning with backpropagation. Decomposition can be argued to serve as a powerful inductive bias to learn useful representations, even though error signals cannot be backpropagated across the whole network. Further, the visual operator that contributes most to the performance improvement depends on the properties of the dataset: LBP for GTSRB and DTCWT for STL10.

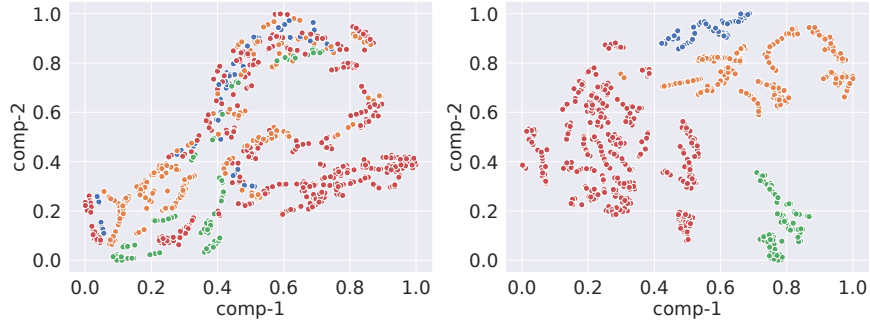


Figure 2: Qualitative results illustrating t-SNE dimensionality reduction of the latent encodings on GTSRB of CLAPP (left plot) and our framework trained locally (right plot) models. We visualize only 4 classes of street signs to avoid clutter. The following classes were randomly chosen: Speed Limit 20km/h sign (blue), Turn Straight Sign (green), No way general sign (orange), Attention bottleneck sign (red). Further visualizations of t-SNE and PCA dimensionality reduction are included in the appendix.

Method	<i>STL10</i>	<i>GTSRB</i>
CLAPP Illing et al. [2021]	66.61 ± 0.28	79.61 ± 0.81
Multi-encoder CLAPP	68.65 ± 0.44	83.81 ± 0.78
ours (Local)	72.97 ± 0.02	94.21 ± 0.24

Table 2: Ablation of the visual invariant operators. Performance comparison in terms of classification accuracy (%)

4.3 t-SNE Visualization

We qualitatively support our empirical classification results (Table 1) by plotting the t-SNE Van der Maaten and Hinton [2008] embedding of the encodings on CLAPP and on our method with decomposition (Figure 2). The plot shows the potential of our decomposition approach in separating representations of different classes. However, we note that separability of t-SNE clusters depends on the chosen dataset and the visualized classes. For instance, the class with speed limit sign 20km/h will form a cluster that is much closer to classes of other speed limit signs. Further visualization on different classes as well as on STL10 dataset can be found in the appendix.

4.4 Ablation Study

We conduct an ablation study to investigate the impact of concatenating the representations of multiple parallel encoders. We train three encoders with CLAPP loss in a similar manner to previous sections and then concatenate their latent representations for prediction. The object classification results are presented in Table 2. Indeed, representation concatenation seems to improve the performance compared to a single encoder, but the performance improvement is not as pronounced as the improvement with the additional operators (2% compared to 6.48% on STL10 and 4% compared to 14% on GTSRB). This further highlights that the improved performance of our proposed network is not primarily due to just multiple encoders but mostly due to strong inductive biases provided by the visual invariant operators.

4.5 Multi-Target Classification

To further understand how of the decomposition approach scales to real world applications, we benchmark our method on the CODEBRIM dataset Mundt et al. [2019]. We train our encoders in a similar manner to previous experiments. After that, we freeze the weights of the encoder and train a linear downstream multi-target classifier on representations created by the frozen encoder (Table 3).

We see that our method leads to a better classification performance on all CODEBRIM classes compared to standard end-to-end models. Our design achieves a multi-target performance that is close to supervised baseline both with local rules and backpropagation. And this is despite training the encoder in a self-supervised setting.

Moreover, we observe that the pipeline with the local learning slightly outperforms the pipeline trained with backpropagation. One possible explanation is that the CODEBRIM dataset is a much smaller dataset than STL10 or GTSRB.

Method	Multi-Target	AvgAcc
Supervised VGG	58.9 ± 0.3	88.87 ± 0.46
MetaQNN-1 Mundt et al. [2019]	66.2 ± 1.6	87.6 ± 0.5
HingeCPC Illing et al. [2021], Oord et al. [2018]	33.87 ± 0.12	82.27 ± 0.27
CLAPP Illing et al. [2021]	37.78 ± 0.5	83.05 ± 0.6
<i>LBP</i> + HingeCPC	23.3 ± 0.18	77.34 ± 0.3
<i>RGNorm</i> + HingeCPC	6.25 ± 0.1	76.2 ± 0.1
<i>DTCWT</i> + HingeCPC	47.2 ± 0.2	84.7 ± 0.4
<i>LBP</i> + CLAPP	20.11 ± 1.5	76.94 ± 0.83
<i>RGNorm</i> + CLAPP	6.25 ± 0.1	76.22 ± 0.1
<i>DTCWT</i> + CLAPP	48.9 ± 0.7	85.5 ± 0.3
ours (Backprop)	53.19 ± 0.5	87.55 ± 0.25
ours (Local)	54.15 ± 0.4	87.79 ± 0.4

Table 3: Performance comparison in terms of multi-target classification and class average accuracy (%) on CODEBRIM test set. Multi-target accuracy refers to classification of all classes correctly in the image. The best performing self-supervised model is highlighted in red, in bold the best performing model for each category: baselines, models trained with HingeCPC, models trained with CLAPP, decomposed encoders.

As observed in previous works Lagani et al. [2021], training with Hebbian rules can in some cases be more sample efficient.

4.6 CODEBRIM with Perturbations

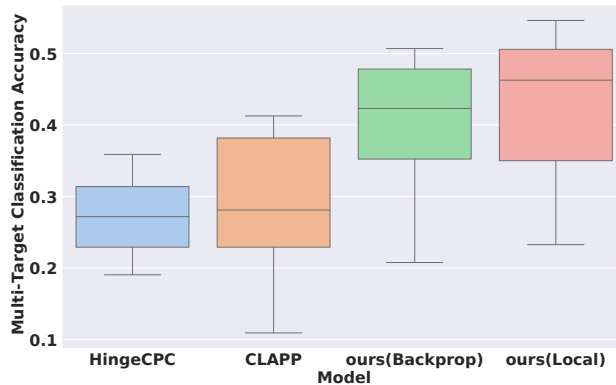


Figure 3: Box plot illustration to summarize the multi-target test classification results under different perturbation settings. Multi-target classification accuracy (%) refers to classification of all classes correctly at the same time. Each box plot shows the median, first and third quartile and minimum and maximum values obtained from all experimental results under different perturbation settings. Further results for each type of perturbation can be found in the appendix.

In this section, we evaluate the robustness of the proposed models to common perturbations. We choose perturbations that can be encountered in real applications. Gaussian noise may appear due to poor illumination or overheated sensors. Motion blur is caused by motion of the camera during acquisition. Planckian Jitter creates realistic physics-based variations in chromaticity Zini et al. [2022]. Shadows and brightness artifacts can occur when capturing data in the wild in the presence of some light source.

We simulate these perturbations on the CODEBRIM data with the Kornia package Riba et al. [2020] and study how the performance degrades across different models, presented in the previous section. Note that our encoders and their corresponding classifiers were not re-trained with these additional perturbations as data augmentations. The models are exposed to these perturbations for the first time during inference on the test set. Our goal is to show how the addition of multiple visual invariant operators can help to mitigate the performance degradation on adversarial examples.

Figure 3 summarizes the multi-target downstream classification performance for different perturbations with different intensities. It appears that overall, decomposition leads to better classification performance on adversarial examples both in the case of the biologically plausible model and the backpropagation model.

Method	Top-1 Acc	Top-5 Acc
Supervised VGG	45.3 ± 0.5	77.2 ± 0.3
HingeCPC Illing et al. [2021], Oord et al. [2018]	33.7 ± 0.18	60.43 ± 0.8
CLAPP Illing et al. [2021]	29.66 ± 0.3	53.81 ± 0.7
<i>LBP</i> +HingeCPC	30.9 ± 0.2	54.7 ± 0.8
<i>RGNorm</i> +HingeCPC	3.74 ± 1.1	14.83 ± 1.4
<i>DTCWT</i> +HingeCPC	26.32 ± 0.86	49.19 ± 0.42
<i>LBP</i> +CLAPP	27.11 ± 1.18	49.93 ± 0.73
<i>RGNorm</i> +CLAPP	5.66 ± 1.33	17.5 ± 1.1
<i>DTCWT</i> +CLAPP	28.7 ± 0.4	50.8 ± 0.8
ours (Backprop)	35.9 ± 0.5	63.4 ± 0.4
ours(Local)	35.41 ± 0.7	62.8 ± 0.6
ours (Backprop)+MovNet	39.67 ± 0.6	68.37 ± 0.25
ours(Local)+MovNet	38.88 ± 0.3	66.28 ± 0.6

Table 4: Performance comparison in terms of classification accuracy (%) on UCF101 test set. The best performing self-supervised model is highlighted in red, in bold the best performing model for each category: baselines, models trained with HingeCPC, models trained with CLAPP, decomposed encoders, decomposed encoders with motion pipeline.

4.7 Experimental Results on Video Streams

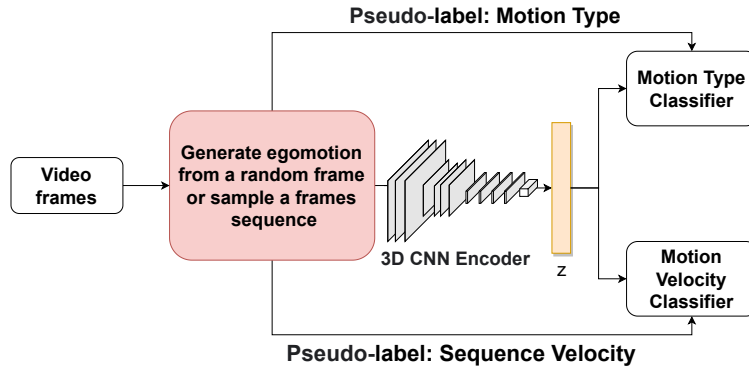


Figure 4: Diagram illustrating the training procedure for motion sensitive neural network (MovNet) on video data. See appendix for further details.

For video data, we extend our framework with another encoder (MovNet) for encoding motion representations. Inspired by previous works on motion representation learning (Mineault et al. [2021], Rideaux and Welchman [2020], Huang et al. [2021]), we propose a self-supervised task to learn motion features from a sequence of frames. Figure 4 illustrates the training procedure. The task is based on the discrimination between egomotion and motion of objects in the scene on one hand, and the prediction of the speed of motion on the other. We hypothesize that if an agent is capable of differentiating between the camera motion and the motion of objects, then it should learn to extract latent representations encoding motion information, which can then be used for a better and more robust action and object recognition in video streams. Egomotion is generated by sampling a single video frame randomly and generating a sequence of overlapping patches. This encoder is trained end-to-end with backpropagation and is included in our experiments to further illustrate how a decomposed design for representation learning can be beneficial in achieving better performance. For further implementation details, see appendix.

The results for the action recognition downstream task are presented in Table 4. The addition of a single decomposition operator leads to worse performance compared to the network without any operators. This contrasts with the self-supervised results for object recognition in previous sections where the inductive bias provided by at least one decomposition operator helps the network learn more linearly separable representation (LBP on GTSRB and DTCWT on STL10 and COBEPRIM). But despite the fact that each single encoder of our framework has a worse performance

than the encoder without any visual operator, the overall framework achieves the best classification accuracy. The proposed combination of operators is flexible enough to achieve better performance compared to baseline encoders.

The framework trained with local learning rules shows more substantial improvement compared to its baseline (6% improvement of ours(Local) compared to CLAPP and 2% improvement for ours(Backprop) compared to HingeCPC). This is consistent with results from the previous sections. Furthermore, adding the encoder trained on motion information to our framework leads to even better performance.

The addition of a motion sensitive module leads to a more linearly separable latent representation as suggested by the better classification performance. These results indicate that motion information can be helpful in action recognition from video data. This also supports our hypothesis that decomposition into multiple parallel representations can alleviate representation learning in different application contexts and on different data forms.

5 Conclusion

In this manuscript, we presented a framework to study the impact of decomposition as an inductive bias on representation learning with local plasticity rules as well as backpropagation. Our experiments indicate that the decomposition of an input signal with well understood image transformation operators can be a powerful tool to learn more generalizable latent representations. Additionally, it can be beneficial to close the gap between representation learning with local rules and backpropagation.

These results showcase the importance of domain knowledge and application context understanding when choosing the decomposition pipeline as each dataset requires different quasi-invariances. Formalization of the choice of operators is an important issue to have stable performance across different domains. A single decomposition operator projects the input signal into a quasi-invariant space and gets rid of some variations of the input which might prove useful to solve a downstream task. Hence, it is crucial that the chosen operators are complementary so that the whole system is able to achieve better performance in different contexts.

6 Acknowledgments

This work was supported by the German Federal Ministry of Education and Research (BMBF) funded projects 01IS19062 "AISEL" and 16DHBKI019 "ALI".

References

- Thomas O Binford and Tod S Levitt. Quasi-invariants: Theory and exploitation. In *Proc. DARPA Image Understanding Workshop*, pages 819–829, 1993.
- Roland T Chin and Charles R Dyer. Model-based recognition in robot vision. *ACM Computing Surveys (CSUR)*, 18(1): 67–108, 1986.
- Yoshua Bengio. Learning deep architectures for ai. *Foundations and Trends® in Machine Learning*, 2(1):1–127, 2009.
- Alex Krizhevsky, Ilya Sutskever, and Geoffrey E Hinton. Imagenet classification with deep convolutional neural networks. In *Advances in Neural Information Processing Systems (NeurIPS)*, volume 25, 2012.
- Yann LeCun, Fu Jie Huang, and Leon Bottou. Learning methods for generic object recognition with invariance to pose and lighting. In *Proceedings of the Computer Vision and Pattern Recognition Conference (CVPR)*, volume 2, pages II–104. IEEE, 2004.
- Artem Moskalev, Anna Sepliarskaia, Ivan Sosnovik, and Arnold Smeulders. LieGG: Studying Learned Lie Group Generators. In *Advances in Neural Information Processing Systems (NeurIPS)*, 2022. URL <http://arxiv.org/abs/2210.04345>.
- Ziming Liu and Max Tegmark. Machine learning hidden symmetries. *Physical Review Letters*, 128(18), 2022. ISSN 10797114. doi:10.1103/PhysRevLett.128.180201.
- Alejandro Barredo Arrieta, Natalia Díaz-Rodríguez, Javier Del Ser, Adrien Bennetot, Siham Tabik, Alberto Barbado, Salvador García, Sergio Gil-Lopez, Daniel Molina, Richard Benjamins, Raja Chatila, and Francisco Herrera. Explainable Artificial Intelligence (XAI): Concepts, taxonomies, opportunities and challenges toward responsible AI. *Information Fusion*, 58:82–115, 2020. ISSN 15662535. doi:10.1016/j.inffus.2019.12.012. URL <https://doi.org/10.1016/j.inffus.2019.12.012>.
- Diogo V. Carvalho, Eduardo M. Pereira, and Jaime S. Cardoso. Machine learning interpretability: A survey on methods and metrics. *Electronics*, 8(832):1–34, 2019. ISSN 20799292. doi:10.3390/electronics8080832.

- Zachary C Lipton. The mythos of model interpretability. In *ICML Workshop on Human Interpretability in Machine Learning*, 2016.
- Neil A Thacker, Adrian F Clark, John L Barron, J Ross Beveridge, Patrick Courtney, William R Crum, Visvanathan Ramesh, and Christine Clark. Performance characterization in computer vision: A guide to best practices. *Computer Vision and Image Understanding*, 109(3):305–334, 2008.
- Anil S. Baslamisli, Yang Liu, Sezer Karaoglu, and Theo Gevers. Physics-based shading reconstruction for intrinsic image decomposition. *Computer Vision and Image Understanding*, 205, 2021. ISSN 1090235X. doi:10.1016/j.cviu.2021.103183.
- Shangzhen Luan, Chen Chen, Baochang Zhang, Jungong Han, and Jianzhuang Liu. Gabor convolutional networks. *IEEE Transactions on Image Processing*, 27(9):4357–4366, 2018. ISSN 10577149. doi:10.1109/TIP.2018.2835143.
- Juan C. Pérez, Motasem Alfarra, Guillaume Jeanneret, Adel Bibi, Ali Thabet, Bernard Ghanem, and Pablo Arbeláez. Gabor layers enhance network robustness. In *Proceedings of the European Conference on Computer Vision (ECCV)*, 2020.
- Leslie G Ungerleider. Two cortical visual systems. *Analysis of visual behavior*, pages 549–586, 1982.
- Christoph von der Malsburg. A vision architecture. *arXiv preprint arXiv: 1407.1642*, 2014.
- Geoffrey Hinton. How to represent part-whole hierarchies in a neural network. *arXiv preprint arXiv:2102.12627*, 2021.
- Jeff Hawkins, Marcus Lewis, Mirko Klukas, Scott Purdy, and Subutai Ahmad. A framework for intelligence and cortical function based on grid cells in the neocortex. *Frontiers in Neural Circuits*, page 121, 2019.
- Donald Olding Hebb. *The organization of behavior: a neuropsychological theory*. Science editions, 1949.
- Roman Pogodin and Peter Latham. Kernelized information bottleneck leads to biologically plausible 3-factor hebbian learning in deep networks. In *Advances in Neural Information Processing Systems (NeurIPS)*, volume 33, pages 7296–7307, 2020.
- Timothy P Lillicrap, Daniel Cownden, Douglas B Tweed, and Colin J Akerman. Random synaptic feedback weights support error backpropagation for deep learning. *Nature Communications*, 7(1):1–10, 2016.
- Erkki Oja. Simplified neuron model as a principal component analyzer. *Journal of mathematical biology*, 15(3): 267–273, 1982.
- Timo Wunderlich, Akos F Kungl, Eric Müller, Andreas Hartel, Yannik Stradmann, Syed Ahmed Aamir, Andreas Grübl, Arthur Heimbrecht, Korbinian Schreiber, David Stöckel, et al. Demonstrating advantages of neuromorphic computation: a pilot study. *Frontiers in Neuroscience*, 13:260, 2019.
- Sergey Bartunov, Adam Santoro, Blake Richards, Luke Marris, Geoffrey E Hinton, and Timothy Lillicrap. Assessing the scalability of biologically-motivated deep learning algorithms and architectures. In *Advances in Neural Information Processing Systems (NeurIPS)*, volume 31, 2018.
- Anthony M Zador. A critique of pure learning and what artificial neural networks can learn from animal brains. *Nature Communications*, 10(1):1–7, 2019.
- Irina Higgins, Loic Matthey, Arka Pal, Christopher Burgess, Xavier Glorot, Matthew Botvinick, Shakir Mohamed, and Alexander Lerchner. beta-VAE: Learning Basic Visual Concepts with a Constrained Variational Framework. In *International Conference on Learning Representations (ICLR)*, 2017. URL <https://openreview.net/forum?id=Sy2fzU9g1>.
- Irina Higgins, Sébastien Racanière, and Danilo Rezende. Symmetry-Based Representations for Artificial and Biological General Intelligence. *Frontiers in Computational Neuroscience*, 16:1–16, 2022. ISSN 16625188. doi:10.3389/fncom.2022.836498.
- Francesco Locatello, Stefan Bauer, Mario Lucie, Gunnar Rätsch, Sylvain Gelly, Bernhard Schölkopf, and Olivier Bachem. Challenging common assumptions in the unsupervised learning of disentangled representations. In *36th International Conference on Machine Learning (ICML)*, volume 2019-June, pages 7247–7283, 2019. ISBN 9781510886988.
- Emile Mathieu, Tom Rainforth, N. Siddharth, and Yee Whye Teh. Disentangling disentanglement in variational autoencoders. In *36th International Conference on Machine Learning (ICML)*, pages 7744–7754, 2019. ISBN 9781510886988.
- Michael Niemeyer and Andreas Geiger. GIRAFFE: Representing scenes as compositional generative neural feature fields. In *Proceedings of the Computer Vision and Pattern Recognition Conference (CVPR)*, pages 11453–11464, 2021. URL <http://arxiv.org/abs/2011.12100>.

- Thu Nguyen-Phuoc, Chuan Li, Lucas Theis, Christian Richardt, and Yong-Liang Yang. HoloGAN: Unsupervised learning of 3D representations from natural images. In *Proceedings of the IEEE/CVF International Conference on Computer Vision (ICCV)*, pages 7588–7597, 2019. ISBN 9781728148038. doi:10.1109/iccvw.2019.00255.
- Florent Perronnin and Diane Larlus. Fisher vectors meet neural networks: A hybrid classification architecture. In *Proceedings of the Computer Vision and Pattern Recognition Conference (CVPR)*, pages 3743–3752, 2015.
- Felix Juefei-Xu, Vishnu Naresh Boddeti, and Marios Savvides. Local binary convolutional neural networks. In *Proceedings of the Computer Vision and Pattern Recognition Conference (CVPR)*, pages 19–28, 2017.
- Jeng Hau Lin, Justin Lazarow, Yunfan Yang, Dezhi Hong, Rajesh K. Gupta, and Zhuowen Tu. Local Binary Pattern Networks. In *IEEE/CVF Winter Conference on Applications of Computer Vision (WACV)*, pages 814–823, 2020. ISBN 9781728165530. doi:10.1109/WACV45572.2020.9093550.
- Joel Dapello, Tiago Marques, Martin Schrimpf, Franziska Geiger, David Cox, and James J DiCarlo. Simulating a primary visual cortex at the front of cnns improves robustness to image perturbations. In *Advances in Neural Information Processing Systems (NeurIPS)*, volume 33, pages 13073–13087, 2020.
- Edouard Oyallon, Eugene Belilovsky, and Sergey Zagoruyko. Scaling the scattering transform: Deep hybrid networks. In *Proceedings of the IEEE international conference on computer vision*, pages 5618–5627, 2017.
- Qiufu Li, Linlin Shen, Sheng Guo, and Zhihui Lai. Wavelet integrated cnns for noise-robust image classification. In *Proceedings of the Computer Vision and Pattern Recognition Conference (CVPR)*, pages 7245–7254, 2020.
- Longlong Jing and Yingli Tian. Self-supervised visual feature learning with deep neural networks: A survey. *arXiv*, pages 1–24, 2019. ISSN 23318422. doi:10.1109/tpami.2020.2992393.
- Phuc H. Le-Khac, Graham Healy, and Alan F. Smeaton. Contrastive representation learning: A framework and review. *IEEE Access*, 8, 2020. doi:10.1109/access.2020.3031549.
- Bernd Illing, Jean Ventura, Guillaume Bellec, and Wulfram Gerstner. Local plasticity rules can learn deep representations using self-supervised contrastive predictions. In *Advances in Neural Information Processing Systems (NeurIPS)*, volume 34, pages 30365–30379, 2021.
- Tang et al. Biologically plausible training mechanisms for self-supervised learning in deep networks. *Front. Comput. Neurosci*, 2022.
- Dmitry Krotov and John J Hopfield. Unsupervised learning by competing hidden units. *Proceedings of the National Academy of Sciences (PNAS)*, 116(16):7723–7731, 2019.
- Arild Nøkland and Lars Hiller Eidnes. Training neural networks with local error signals. In *International Conference on Machine Learning (ICML)*, pages 4839–4850. PMLR, 2019.
- Xiaohui Xie and H Sebastian Seung. Equivalence of backpropagation and contrastive hebbian learning in a layered network. *Neural Computation*, 15(2):441–454, 2003.
- Beren Millidge, Yuhang Song, Tommaso Salvatori, Thomas Lukasiewicz, and Rafal Bogacz. Backpropagation at the infinitesimal inference limit of energy-based models: Unifying predictive coding, equilibrium propagation, and contrastive hebbian learning. *arXiv preprint arXiv: 2206.02629*, 2022.
- Yali Amit. Deep learning with asymmetric connections and hebbian updates. *Frontiers in Computational Neuroscience*, 13:18, 2019.
- Brian Crafton, Abhinav Parihar, Evan Gebhardt, and Arijit Raychowdhury. Direct feedback alignment with sparse connections for local learning. *Frontiers in Neuroscience*, 13:525, 2019.
- Donghyeon Han and Hoi-jun Yoo. Efficient convolutional neural network training with direct feedback alignment. *arXiv preprint arXiv: 1901.01986*, 2019.
- Theodore H Moskovitz, Ashok Litwin-Kumar, and LF Abbott. Feedback alignment in deep convolutional networks. *arXiv preprint arXiv: 1812.06488*, 2018.
- Arild Nøkland. Direct feedback alignment provides learning in deep neural networks. In *Advances in Neural Information Processing Systems (NeurIPS)*, volume 29, 2016.
- Gabriele Lagani, Fabrizio Falchi, Claudio Gennaro, and Giuseppe Amato. Hebbian semi-supervised learning in a sample efficiency setting. *Neural Networks*, 143:719–731, 2021.
- Peter Földiák. Forming sparse representations by local anti-hebbian learning. *Biological Cybernetics*, 64(2):165–170, 1990.
- Timo Ojala, Matti Pietikainen, and Topi Maenpää. Multiresolution gray-scale and rotation invariant texture classification with local binary patterns. *IEEE Transactions on Pattern Analysis and Machine Intelligence*, 24(7):971–987, 2002.

- TI Maenpaa. *The local binary pattern approach to texture analysis: Extensions and applications*. PhD thesis, University of Oulu, Finland, 2004.
- Timo Ahonen, Abdenour Hadid, and Matti Pietikainen. Face description with local binary patterns: Application to face recognition. *IEEE Transactions on Pattern Analysis and Machine Intelligence*, 28(12):2037–2041, 2006.
- Theo Gevers and Arnold W.M. Smeulders. Color-based object recognition. *Pattern Recognition*, 32(3):453–464, 1999. ISSN 0031-3203. doi:[https://doi.org/10.1016/S0031-3203\(98\)00036-3](https://doi.org/10.1016/S0031-3203(98)00036-3). URL <https://www.sciencedirect.com/science/article/pii/S0031320398000363>.
- Nick G Kingsbury. The dual-tree complex wavelet transform: a new technique for shift invariance and directional filters. In *IEEE Digital Signal Processing Workshop*, volume 86, pages 120–131. Citeseer, 1998.
- Joan Bruna and Stéphane Mallat. Invariant scattering convolution networks. *IEEE transactions on pattern analysis and machine intelligence*, 35(8):1872–1886, 2013.
- Clemens Valens. A really friendly guide to wavelets. *ed. Clemens Valens*, 1999.
- Aaron van den Oord, Yazhe Li, and Oriol Vinyals. Representation learning with contrastive predictive coding. *arXiv preprint arXiv: 1807.03748*, 2018.
- Johannes Stallkamp, Marc Schlipsing, Jan Salmen, and Christian Igel. The german traffic sign recognition benchmark: a multi-class classification competition. In *International Joint Conference on Neural Networks*, pages 1453–1460. IEEE, 2011.
- Adam Coates, Andrew Ng, and Honglak Lee. An analysis of single-layer networks in unsupervised feature learning. In *Proceedings of the fourteenth International Conference on Artificial Intelligence and Statistics*, pages 215–223. JMLR Workshop and Conference Proceedings, 2011.
- Martin Mundt, Sagnik Majumder, Sreenivas Murali, Panagiotis Panetsos, and Visvanathan Ramesh. Meta-learning convolutional neural architectures for multi-target concrete defect classification with the concrete defect bridge image dataset. In *Proceedings of the Computer Vision and Pattern Recognition Conference (CVPR)*, pages 11196–11205, 2019.
- Khurram Soomro, Amir Roshan Zamir, and Mubarak Shah. Ucf101: A dataset of 101 human actions classes from videos in the wild. *arXiv preprint arXiv: 1212.0402*, 2012.
- Sindy Löwe, Peter O’Connor, and Bastiaan Veeling. Putting an end to end-to-end: Gradient-isolated learning of representations. In *Advances in Neural Information Processing Systems (NeurIPS)*, volume 32, 2019.
- Laurens Van der Maaten and Geoffrey Hinton. Visualizing data using t-sne. *Journal of Machine Learning Research*, 9(11), 2008.
- Simone Zini, Marco Buzzelli, Bartłomiej Twardowski, and Joost van de Weijer. Planckian jitter: enhancing the color quality of self-supervised visual representations. *arXiv preprint arXiv: 2202.07993*, 2022.
- Edgar Riba, Dmytro Mishkin, Daniel Ponsa, Ethan Rublee, and Gary Bradski. Kornia: an open source differentiable computer vision library for pytorch. In *IEEE/CVF Winter Conference on Applications of Computer Vision (WACV)*, pages 3674–3683, 2020.
- Patrick Mineault, Shahab Bakhtiari, Blake Richards, and Christopher Pack. Your head is there to move you around: Goal-driven models of the primate dorsal pathway. In *Advances in Neural Information Processing Systems (NeurIPS)*, volume 34, pages 28757–28771, 2021.
- Reuben Rideaux and Andrew E Welchman. But still it moves: static image statistics underlie how we see motion. *Journal of Neuroscience*, 40(12):2538–2552, 2020.
- Ziyuan Huang, Shiwei Zhang, Jianwen Jiang, Mingqian Tang, Rong Jin, and Marcelo H Ang. Self-supervised motion learning from static images. In *Proceedings of the Computer Vision and Pattern Recognition Conference (CVPR)*, pages 1276–1285, 2021.